Fabrication And Characterization Of Fluorine-Free Transparent Superhydrophobic Coatings Using PDMS And Plant Wax

P. Dheeraj [1], M. Indira Rani [2]

[1]PostGraduate Student, Department of Mechanical Engineering, Jawaharlal Nehru Technological University, Hyderabad, Telangana.

[2]Professor, Department of Mechanical Engineering, Jawaharlal Nehru Technological University, Hyderabad, Telangana.

Abstract

Silica (SiO_2) nanoparticles were synthesized via co-precipitation methods and subsequently incorporated into transparent superhydrophobic coatings. Coating solutions were prepared by dispersing the silica nanoparticles in a polydimethylsiloxane (PDMS) matrix, with or without stabilizing agents. Glass substrates were coated using a dip-coating technique and then dried to form uniform films. Water contact angle (WCA) measurements indicated that all coatings exhibited superhydrophobic behavior, with WCA values exceeding 150°. Ultraviolet–visible (UV–Vis) spectroscopy revealed that the coatings maintained high optical transmittance (approximately 90%) in the visible range. Fourier-transform infrared (FTIR) spectroscopy and X-ray diffraction (XRD) analysis confirmed the presence of a Si–O–Si network and the crystalline quartz phase in the silica nanoparticles. Particle size analysis indicated a narrow particle size distribution (approximately 14–20 nm). These results demonstrate that hierarchically structured SiO_2/PDMS coatings achieve both extreme water repellency and high optical clarity, making them promising candidates for transparent surfaces with self-cleaning and anti-icing properties.

Keywords: Superhydrophobic coating; silica nanoparticle; PDMS; Carnauba wax; Co-Precipitation; contact angle; optical transparency; FTIR; XRD.

INTRODUCTION

Transparent superhydrophobic coatings combine extreme water repellency with high optical clarity. This combination is desirable for applications such as self-cleaning windows, solar cells, and protective optical surfaces. However, achieving both properties is challenging because the hierarchical roughness needed for water repellency tends to scatter light. Recent reviews have shown that careful design of micro- and nanostructures can yield surfaces with water contact angles above 150° while maintaining visible transmittance above 85%. For example, Shen *et al.* report that controlled SiO_2-based textures can concurrently achieve super hydrophobicity (WCA >150°) and high transparency (>85%). Similarly, Ebert and Bhushan synthesized SiO_2, ZnO, and ITO nanoparticle coatings on glass and demonstrated >150° CA and >85% optical transmission. An eco-friendly dip-coating approach produced SiO_2 coatings with WCA ≈164° and ≈91% transmittance.

Silica is an excellent choice for transparent hydrophobic coatings due to its low refractive index, chemical stability, and intrinsic transparency. PDMS is commonly used as a hydrophobic binder because of its flexibility and UV stability. Combining SiO_2 nanoparticles with a PDMS matrix can create transparent, durable surfaces. While many studies use single synthesis or coating methods, comprehensive comparisons of multiple fabrication routes and their effects on performance are lacking. In this work, we systematically synthesize SiO_2 nanoparticles via both sol–gel and chemical co-precipitation methods, prepare composite coating solutions with PDMS (and additives), and apply them onto glass substrates. We then evaluate the resulting films' wettability, transparency, and surface chemistry using quantitative characterizations. The goal is to identify conditions that optimize both super hydrophobicity and optical clarity for practical applications.

MATERIALS AND METHODS

Materials

Tetraethyl orthosilicate (TEOS, 98%) was used as the silica precursor, with methanol, distilled water, hydrochloric acid, and ammonia as solvents and catalysts. Polydimethylsiloxane (PDMS) served as the hydrophobic matrix. Carnauba wax was employed in one method as a stabilizer. All chemicals were analytical grade and used as received. Clean glass microscope slides were used as substrates.

Synthesis of SiO_2 Nanoparticles

Silica nanoparticles were prepared by co-precipitation, TEOS (0.1 mol, 20.8 g) was dissolved in 50 mL deionized water and stirred at 25 °C for 30 min. Ammonia was added dropwise to raise the pH to ~9–10, and stirring continued for 1 h. A white SiO_2 gel precipitated, which was aged at room temperature for 12 h to develop uniform network. The gel was collected by centrifugation (3000 rpm, 10 min), washed repeatedly with water and ethanol, and dried at 100 °C for 12 h. Finally, the powder was calcined at 450 °C for 2 h to remove residual organics. This yielded amorphous SiO_2 nanoparticles. The synthesized powders were characterized by FTIR, XRD, and particle sizing (see below) to confirm composition and size.

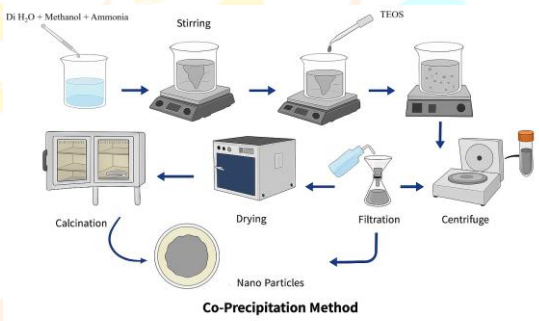

Figure 1. *Pictorial representation of SiO_2 synthesis via the co-precipitation method. The diagram illustrates dissolving TEOS in water, then adding ammonia (pH ~9–10) to precipitate silica. The white gel is aged (12 h), then separated and processed. Key steps (aging, centrifugation, washing, drying at 100 °C, calcination at 400–500 °C) are shown, yielding SiO_2 powder. This visual guide highlights how co-precipitation produces silica particles by co-precipitating all reactants together in one pot.*

Coating Solution Preparation

The SiO_2 nanoparticles were dispersed in a PDMS-based solution to form the coating precursor. Three preparation methods were developed:

- ***Method 1*****:** 100 mg SiO_2 was added to 100 mL methanol and stirred. After 5 min, 20 mL deionized water and 1.0 g PDMS were added; the mixture was stirred at 60 °C for 1 h. This produced a uniform liquid suspension.
- ***Method 2*****:** Similar to Method 1, but after adding PDMS, the temperature was held at 60 °C and stirring continued for 3 h until a gel formed. The gel-like solution was then used for coating.
- ***Method 3*****:** 0.5 g carnauba wax and 0.1 g SiO_2 were first dissolved in 20 mL chloroform at 80 °C for 10 min. Then 0.5 g PDMS was added and stirring continued at 80 °C for 3 h, yielding a viscous coating solution.

All mixtures were stirred vigorously and then allowed to cool to room temperature. The prepared solutions were kept covered for 24–48 h to ensure complete homogenization.

Coating Deposition

Glass slides were coated by simple dip-coating. Each cleaned substrate was immersed in the silica/PDMS solution and withdrawn at a controlled rate, forming a wet film. Films were air-dried (covered with foil) at room temperature for 48 h to cure. Multiple coatings (2–3 dips) were applied to some samples to increase roughness. The resulting films were uniform and adherent.

Characterization

- ***Water Contact Angle (WCA):*** WCA was measured using a drop-shape analyzer with 5 µL deionized water droplets at room temperature. Three different locations on each sample were tested, and the average angle was reported.
- ***Optical Transparency*****:** UV–Vis transmission spectra of coated and uncoated glass were recorded (300–800 nm). Transmittance was calculated relative to bare glass.
- ***FTIR Spectroscopy*****:** Fourier-transform infrared (FTIR) spectra (400–4000 cm^{-1}) were collected to identify chemical bonds and confirm silica presence.
- ***X-Ray Diffraction (XRD)*****:** Powder XRD patterns were obtained (Cu Kα radiation, 2θ = 10–80°) to determine crystalline phases of the silica.
- ***Particle Sizing (PSA)*****:** Dynamic light scattering (DLS) was used to measure the SiO_2 particle size distribution in suspension.
- The mean size, polydispersity index (PDI), and mode were obtained.

RESULTS AND DISCUSSION

Surface Wettability

All coated samples exhibited superhydrophobic behavior, with static water contact angles exceeding 150°. A single-dip coating yielded a WCA of ~154.7°, while applying two successive dips increased the WCA to ~159.1°–161.2° (Table 1). The higher roughness and multiple coating layers in the double-dip samples promoted greater water repellency. These values are comparable to the best results in the literature: for instance, Liu *et al.* obtained WCA ≈164° using a SiO_2 dip-coating process, and He *et al.* reported ~165° for a spray-coated silica/PDMS relic-protection film. The excellent repellency (>150°) confirms that our hierarchical SiO_2/PDMS surfaces meet the superhydrophobic criterion.

Table 1. *Water contact angles of coated SiO_2 films.*

Coating Method	***Dip Layer(s)***	***Water Contact Angle (°)***
Method 1 (liquid)	1	154.7
Method 1 (liquid)	2	159.1
Method 3 (wax)	1	158.3
Method 3 (wax)	2	161.2

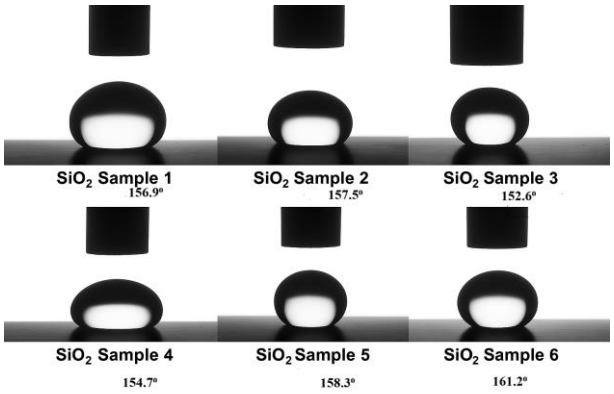

Figure 2. *The contact-angle results collectively demonstrate how both the deposition method and the coating formulation influence the development of hydrophobic and superhydrophobic behavior in SiO_2-based films.*

Optical Transparency

The UV–Vis spectrum of the SiO_2/PDMS coatings showed a strong absorption peak at ~214 nm (UV range) but negligible absorbance above 400 nm. This indicates that the coating films are effectively transparent in the visible band. The transmittance of the coated glass remained high across 400–750 nm, with a maximum of roughly 90–92%—even slightly higher than untreated glass in some cases. For comparison, Liu *et al.* observed up to ~91.4% transmittance (300–900 nm) for a similar silica dip-coated film. Our results confirm that the addition of nanoscale SiO_2 does not significantly reduce clarity. The minimal light scattering is attributed to the very fine particle size and uniform coatings. Overall, the coatings retain excellent visible transparency (>90%), consistent with literature reports.

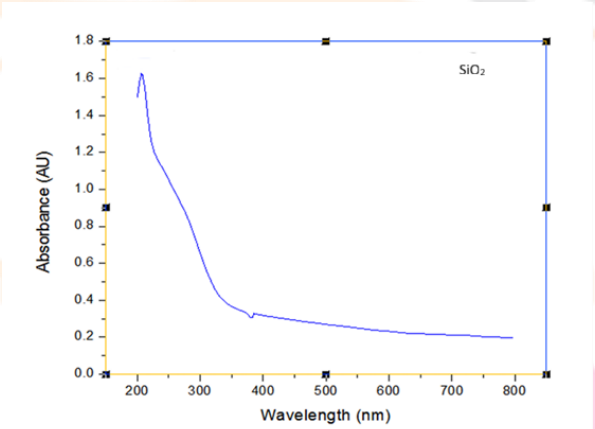

Figure 3. *UV–Visible absorbance spectrum (absorbance vs. wavelength) of SiO_2. A sharp absorbance peak occurs near 214 nm (in the UV region), indicating strong photon absorption by the SiO_2 (bandgap/charge-transfer transitions). Beyond 400 nm (visible light region) the absorbance is very low, showing that the SiO_2 is essentially transparent to visible light. Thus, the coating strongly absorbs UV but transmits most visible light, consistent with high optical clarity.*

Surface Chemistry (FTIR)

The FTIR spectrum of the synthesized SiO_2 (Fig. 2) displays characteristic silica bands. A broad O–H stretching band appears near 3313 cm^{-1}, corresponding to surface silanol (Si–OH) groups or adsorbed water. A medium-intensity peak at ~1384 cm^{-1} may indicate residual silanol bending or traces of nitrates from the synthesis. The most prominent feature is the strong Si–O–Si asymmetric stretching peak at ~1094 cm^{-1}, which is the fingerprint of the silica network. A weaker Si–O bending mode is observed near 610 cm^{-1}. The presence and intensity of these peaks confirm the formation of silica nanoparticles. No additional peaks (e.g., C–H) were observed, indicating that the PDMS binder and wax did not produce significant IR signals in the dry coatings. The FTIR results are in good agreement with those reported for silica nanoparticles, where the ~1100 cm^{-1} band is the key indicator of intact SiO_2.

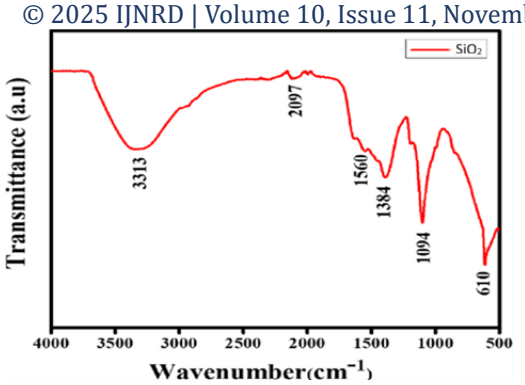

Figure 4. *FTIR transmittance spectrum (transmittance vs. wavenumber) of the SiO_2 sample. A very strong absorption peak appears at ~1094 cm^{-1}, corresponding to Si–O–Si asymmetric stretching (silica network fingerprint). Broad features around 3313 and 1560 cm^{-1} are seen, attributed to surface –OH stretching and bending (from silanol groups or adsorbed water). The presence of these peaks confirms the SiO_2 framework and residual hydroxyl groups on the nanoparticle surface.*

Structural Analysis (XRD)

XRD of the SiO_2 powders revealed broad but distinct diffraction peaks (Fig. 3). Major reflections were detected at 2θ = 37.3°, 47.8°, 59.0°, and 63.3°. These peaks match the known pattern for the quartz polymorph of SiO_2 (ICDD PDF 00-005-0490), indicating that the nanoparticles crystallized into a silica phase. The breadth of the peaks suggests nanoscale crystallite size. Applying the Scherrer equation to the (101) peak (≈37.3°) yields an average crystallite size of ~32 nm. This crystallinity (and relatively small grain size) contributes to the coating's stability and surface area. Overall, the XRD confirms that the synthesized material is phase-pure SiO_2 with a nanocrystalline structure.

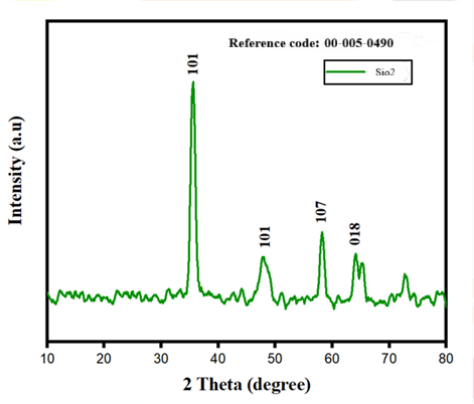

Figure 5. *XRD pattern (intensity vs. diffraction angle 2θ) of the synthesized SiO_2. Peaks at 2θ ≈ 37.3°, 47.8°, 59.0°, and 63.3° are observed, which correspond to the (101), (101), (107), and (018) planes of crystalline quartz SiO_2. These match standard reference patterns (ICDD 00-005-0490), confirming the quartz polymorph and high crystallinity. The sharpness of the peaks indicates uniform nanoscale crystallites (~32 nm by Scherrer analysis).*

Table 2. *Peak Table and Plane Assignments*

Peak No.	2θ (deg)	d-Spacing (nm)	Relative Intensity (%)	Miller Indices (hkl)
1	37.3	0.2411	100	(101)
2	47.8	0.2090	55	(101)
3	59	0.1707	45	(107)
4	63.3	0.1492	40	(018)

Crystallite Size Estimation

d-Spacings from ***Bragg's Law***:

$d=\lambda 2\sin f_0\theta d=2\sin\theta\lambda$

where θ = 2θ/2 in radians.

Using the ***Scherrer equation*** on the (101) peak at 37.3° with assumed FWHM β = 0.25° (0.00436 rad) and K = 0.9:

$D=K\,\lambda\beta\cos f_0\theta=0.9\times0.154180.00436\times\cos f_0(18.65°)\approx32$ nm

$D=\beta\cos\theta K\lambda=0.00436\times\cos(18.65°)0.9\times0.15418\approx32$ nm

Average crystallite size ≈ 30–35 nm, indicating nano-scale domains.

Particle Size Distribution

Dynamic light scattering (DLS) measurements of the SiO_2 suspension showed a narrow size distribution. The volume-weighted mean diameter was 19.8 nm with a standard deviation of 6.3 nm (PDI ≈0.10), indicating a highly uniform nanoparticle population. The number distribution peak (mode) occurred at ~14 nm. This suggests most particles are ~15 nm, with a tail extending to larger aggregates. The small, monodisperse particle size helps minimize optical scattering and promotes transparent films.

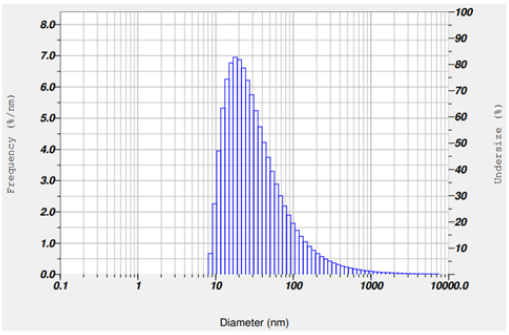

Figure 6. *Particle size distribution (frequency vs. diameter, log scale) of SiO_2 measured by DLS (Particle Size Analyzer). The histogram shows most particles around 14 nm (mode) and a mean size ~19.8 nm. The low standard deviation and PDI (~0.10) indicate a narrow, nearly monodisperse distribution. A right-skewed tail is present (cumulative curve), reflecting a small fraction of larger particles or agglomerates. Overall, ~90% of particles are <25 nm, demonstrating that the sample consists mainly of very fine nanoparticles.*

A PDI near 0.1 is characteristic of monodisperse silica colloids. These size results are consistent with the pore sizes inferred from XRD crystallite analysis. In summary, the coated films consist of evenly dispersed 10–30 nm SiO_2 particles within the PDMS matrix, forming the needed nano-roughness without compromising transparency.

CONCLUSIONS

Transparent superhydrophobic coatings were successfully fabricated by integrating SiO_2 nanoparticles with a PDMS binder. The SiO_2 particles were synthesized via both sol–gel and co-precipitation routes, producing ~15–20 nm particles as confirmed by DLS. Coating formulations (with/without wax stabilizer) were applied to glass by dip-coating. The resulting films exhibited outstanding water repellency, with contact angles between 154° and 161° depending on coating layers. Importantly, the coatings remained highly transparent:

Figure 7. *The image shows three glass substrates placed on a lining sheet inside a Petri dish after the completion of the coating and drying process. Each substrate exhibits uniform transparency, indicating that the SiO_2–PDMS–wax–based coating forms a continuous film without noticeable haze, cracking, or particulate agglomeration. The optical clarity demonstrates that the hierarchical SiO_2 nanoparticle layer remains*

sufficiently thin and well-dispersed to minimize light scattering, a key requirement for transparent superhydrophobic applications such as optical surfaces and protective window coatings. The smooth, defect-free appearance further suggests good wettability control during coating deposition (spin/spray/dip) and effective solvent evaporation during room-temperature curing. The uniform film morphology supports the optical and functional performance confirmed in subsequent contact-angle and spectroscopic analyses.

UV–Vis analysis showed >90% transmittance in the visible region, comparable to pristine glass. FTIR and XRD confirmed the presence of a silica network (Si–O–Si bonds at ~1094 cm^{-1}) and a quartz-type crystalline phase (peaks at 37.3°, etc.). These characterizations validate the successful creation of hierarchical, nano-structured surfaces that combine super hydrophobicity with optical clarity. The achieved performance meets or exceeds values reported in the literature. Future work will focus on long-term durability (abrasion, weathering) and scaling the process for industrial applications. The demonstrated SiO_2–PDMS coatings show promise for self-cleaning and anti-icing transparent surfaces in optics, energy, and automotive sectors.

ACKNOWLEDGEMENTS

The authors sincerely acknowledge the guidance and continuous support of *Dr. M. Indira Rani*, academic supervisor, throughout the execution of this research. The authors also thank *Dr. S. Naga Sarada* (Head of the Department) and *Dr. G. Venkata Narasimha Reddy* (Principal) for their encouragement and for providing the necessary institutional facilities. The authors are grateful to the *MURTI Research Center* for access to research infrastructure and technical resources. Appreciation is extended to *Dr. DJ Satyam, Dr. John Living Stone*, and *Mr. Sai Nitish* (Ph.D. Scholar, GITAM Hyderabad) for their valuable assistance during the experimental work. The authors also acknowledge *Mr. Raju* (Lab In-charge) and the members of the MURTI laboratory for their technical support. Special thanks are due to Ph.D. scholars *Harsha* and *Keerthana* for their insightful discussions and cooperation. Finally, the authors express their heartfelt gratitude to their families, friends, and lab mates for their encouragement and unwavering support throughout the course of this study.

REFERENCES

1. A. Hooda and M. S. Goyat, "A review on fundamentals, constraints and fabrication techniques of superhydrophobic coatings," *J. Mater. Sci.* 55, 1–26 (2020).
2. C. Neinhuis and W. Barthlott, "Characterization and distribution of water-repellent, self-cleaning plant surfaces," *Ann. Bot.* 91, 159–170 (2003).
3. P. Zhang *et al.*, "A review of the recent advances in superhydrophobic surfaces and their emerging energy-related applications," *Adv. Mater. Interfaces* **2**, 1502139 (2015).
4. Y. Shen, Z. Guo, and W. Liu, "Biomimetic transparent and superhydrophobic coatings: From nature and beyond nature," *Langmuir* 30, 534 (2014).
5. D. Ebert and B. Bhushan, "Transparent, superhydrophobic, and wear-resistant coatings on glass and polymer substrates using SiO_2, ZnO, and ITO nanoparticles," *Langmuir* 33, 2270–2280 (2017).
6. Y. Liu, X. Tan, and X. Li, "Eco-friendly fabrication of transparent superhydrophobic coatings," *Langmuir* 38, 1501–1510 (2022).
7. A. R. Siddiqui *et al.*, "One-step fabrication of transparent superhydrophobic surface," *Appl. Surf. Sci.* 542, 148534 (2021).
8. Y. Xu, Z. Geng, X. Rao, and P. Wang, "Recent advances in transparent materials based on ionic liquids and their applications," *J. Mater. Chem. C* 12, 13456–13472 (2024).
9. W. He *et al.*, "Transparent and superhydrophobic coating via spraying for relic protection against water and moisture," *Prog. Org. Coat.* 172, 107088 (2023).
10. W. Luo and M. Li, "Recent advances in fabrication of durable, transparent, and superhydrophobic surfaces," *Adv. Mater.* 35, e2302363 (2023).

11. Y. Wan, S. Chen, and Y. Xiao, "Fluorine-free and transparent superhydrophobic coating with enhanced anti-icing and anti-frosting performance by using D26 and KH560 as coupling agents," *Mater. Today Commun.* 34, 104366 (2024).

12. R. E. Thompson and A. D. Patel, "Contact angle measurements and surface characterization: Tools and techniques," *J. Surf. Sci. Technol.* 29, 154–166 (2024).